

Targeted live-cell nuclear delivery of the DNA ‘light-switching’ Ru(II) complex via ion-pairing with chlorophenolate counter-anions: the critical role of binding stability and lipophilicity of the ion-pairing complexes

Xi-Juan Chao^{1,2}, Miao Tang¹, Rong Huang¹, Chun-Hua Huang¹, Jie Shao¹, Zhu-Ying Yan¹ and Ben-Zhan Zhu^{1,3,4,*}

¹State Key Laboratory of Environmental Chemistry and Ecotoxicology, Research Center for Eco-Environmental Sciences, and University of Chinese Academy of Sciences, The Chinese Academy of Sciences, Beijing 100085, P. R. China, ²MOE Key Laboratory of Bioinorganic and Synthetic Chemistry, School of Chemistry, Sun Yat-Sen University, Guangzhou 510275, P. R. China, ³Linus Pauling Institute, Oregon State University, Corvallis, OR 97331, USA and ⁴Joint Institute for Environmental Science, Research Center for Eco-Environmental Sciences and Hong Kong Baptist University, Hong Kong

Received January 3, 2018; Revised February 18, 2019; Editorial Decision February 19, 2019; Accepted October 02, 2019

ABSTRACT

We have found recently that nuclear uptake of the cell-impermeable DNA light-switching Ru(II)-polypyridyl cationic complexes such as [Ru(bpy)₂(dppz)]Cl₂ was remarkably enhanced by pentachlorophenol (PCP), by forming ion-pairing complexes via a passive diffusion mechanism. However, it is not clear whether the enhanced nuclear uptake of [Ru(bpy)₂(dppz)]²⁺ is only limited to PCP, or it is a general phenomenon for other highly chlorinated phenols (HCPs); and if so, what are the major physicochemical factors in determining nuclear uptake? Here, we found that the nuclear uptake of [Ru(bpy)₂(dppz)]²⁺ can also be facilitated by other two groups of HCPs including three tetrachlorophenol (TeCP) and six trichlorophenol (TCP) isomers. Interestingly and unexpectedly, 2,3,4,5-TeCP was found to be the most effective one for nuclear delivery of [Ru(bpy)₂(dppz)]²⁺, which is even better than the most-highly chlorinated PCP, and much better than its two other TeCP isomers. Further studies showed that the nuclear uptake of [Ru(bpy)₂(dppz)]²⁺ was positively correlated with the binding stability, but to our surprise, inversely correlated with the lipophilicity of the ion-pairing complexes formed between [Ru(bpy)₂(dppz)]Cl₂ and HCPs. These findings should provide new perspectives

for future investigations on using ion-pairing as an effective method for delivering other bio-active metal complexes into their intended cellular targets.

INTRODUCTION

A large number of organometallic transition metal-based complexes have been designed and researched ever since certain platinum complexes were found to be anti-cancer drugs by forming adducts with DNA (1–8). The use of large, planar aromatic systems as DNA intercallators has been well established in chemical and biological studies of DNA and related systems, and dipyrrodo[3,2-a:2',3'-c]phenazine (dppz) has become a standard ligand in the design of metallo-intercallators (9). Ru(II) polypyridyl complexes have unique photophysical properties including intense luminescence, large Stokes shifts, red emission wavelengths and a good photostability (9,10), which make them potentially invaluable for applications in cellular imaging, photochemotherapy, photoswitching, solar energy conversion and photocatalysis (11–15). In the field of luminescent dppz complexes for DNA binding studies, Ru(II) polypyridyl complexes with the general formula [Ru(N^N)₂(dppz)]Cl₂ have been widely applied and studied both experimentally and theoretically due to their strong interactions with DNA (1,2,16–18). Due to complex modulation of the nature of the excited states, it is possible to achieve up to 10⁴ enhancement of emission intensity upon DNA binding compared to the free aqueous species (19), which is advantageous for use in fluorescence microscopy.

*To whom correspondence should be addressed. Tel: +86 10 6284 9030; Fax: +86 10 6292 3563; Email: bzhu@rcees.ac.cn

While there are many studies on the applications of such Ru–dppz complexes, the application in live-cell DNA imaging is rare, due to complications relating to cellular uptake and distribution of such species (16–20). With the characteristic for living cell uptake seemingly established (17–23), numerous studies aimed at effecting membrane permeability by increasing hydrophobicity through hydrophobic ligands, such as DIP (4, 7-diphenyl-1, 10-phenanthroline), or by the addition of alkyl chains or cell penetrating units (e.g. polyarginines) (16,17,21,22), which are more ‘lipid-like’ in nature, have been carried out. However, while change in hydrophobicity can modulate cellular uptake, it can also affect cellular localization of these complexes and can often lead to a decrease in nuclear targeting, which will limit their applicability as *in vivo* DNA probes.

Lipophilicity has been considered to be responsible for the cellular uptake of Ru(II) polypyridyl complexes (16,17). During our study on the mechanism of synergistic biochemical and toxicological effects between organic and inorganic compounds (especially transition metal complexes) (24–32), we found recently, that nuclear uptake of the cell-impermeable Ru(II)-polypyridyl complexes such as [Ru(bpy)₂(dppz)]Cl₂ was remarkably enhanced by pentachlorophenol (PCP) and two other biochemical agents, by forming lipophilic and relatively stable ion-pairing complexes via a passive diffusion mechanism (33). However, it is not clear whether the enhanced nuclear uptake of [Ru(bpy)₂(dppz)]²⁺ is only limited to PCP, or it is a general phenomenon for other highly chlorinated phenols (HCPs) as well; and if so, what are the major physicochemical factors in determining nuclear uptake? In this study, we found that the cellular and nuclear uptake of [Ru(bpy)₂(dppz)]²⁺ can also be facilitated by two other groups of HCPs including three tetrachlorophenols (TeCPs) and six trichlorophenols (TCPs). Interestingly and unexpectedly, the most effective nuclear uptake of Ru was facilitated by 2,3,4,5-TeCP, one of the three less chlorinated TeCP isomers, not by the most highly chlorinated PCP. Further studies showed that the efficiency in facilitating cellular uptake of Ru(II)-dppz complexes for HCPs was positively correlated with the binding ability, but to our surprise, inversely correlated with the lipophilicity of the ion-pairing complexes formed between [Ru(bpy)₂(dppz)]Cl₂ and HCPs. These findings may have important implications in future investigations on delivering other bio-active metal complexes into their intended cellular targets via ion-pairing method.

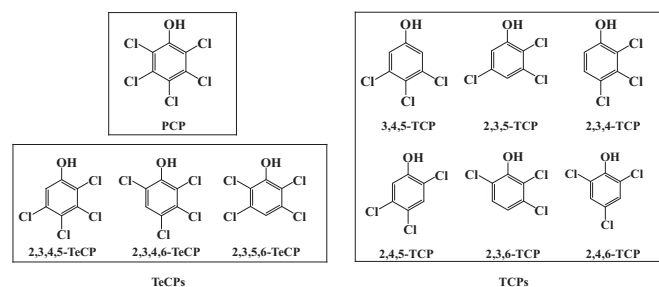
MATERIALS AND METHODS

Chemicals

The [Ru(bpy)₂(dppz)]Cl₂ (Scheme 1) complex was synthesized according to (34–36). HCPs were purchased from Sigma.

Cell culture

HeLa cells were cultured in Dulbecco’s modified Eagle’s medium (DMEM) medium with 10% fetal bovine serum and 1% penicillin-streptomycin, at 37°C under a 5% CO₂ atmosphere. Cells for confocal imaging were seeded on round



Scheme 1. Chemical structures of three groups of highly chlorinated phenols (HCPs); PCP: pentachlorophenol; TeCPs: tetrachlorophenols; TCPs: trichlorophenols.

coverslips at a density of ~100 000 cells/coverslip and cultured for 1 day.

Partitioning study

Organic solvent (n-octanol)/aqueous (Tris–HCl buffer, 10 mM, pH 7.4) phase partition for Ru(II) complexes in the presence or absence of bio-chemical agents, were conducted using the ‘shake-flask’ method, with the concentration in each phase determined by UV-vis absorbance (Beckman DU-800).

Flow cytometry

HeLa cells were detached from monolayer culture with trypsin, re-suspended in medium with serum and diluted to 1×10^6 cells/ml. The complex [Ru(bpy)₂(dppz)]Cl₂ (100 μM) and HCPs (300 μM) were added to the cells, successively. The cells were isolated by centrifugation and rinsed with cold phosphate buffered saline (PBS) for three times. Flow cytometry was performed on a BD FACS Caliber using ~20 000 cells per sample. Luminescence data were obtained by excitation of 488 nm with emission at 600–630 nm for Ru(II) complexes.

Confocal laser scanning microscopy

After incubated with the Ru(II) complex and chlorinated phenols, cells were rinsed with PBS for three times, and were luminescently imaged on a confocal laser scanning microscopy (CLSM) using 40× oli-immersion lens for slide imaging. The imaging was excited with 488 nm and emission was monitored at 600–630 nm. All cells were washed with PBS before imaging. Microscopy was performed on a Leica TCS SP5 CLSM. Live cells were distinguished by their low To-Pro-3 emission with excitation at 633 nm and observation at 650–670 nm.

ICP-MS analysis

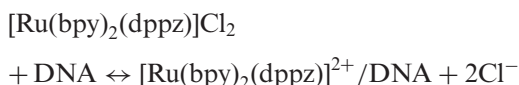
Exponentially growing HeLa cells were plated at a density of 0.5×10^6 cells/ml in DMEM medium. Ruthenium complexes (final concentration 100 μM) were added to the culture medium and incubated for 1 h at 37°C with 5% CO₂. After digestion in trypsin–ethylenediaminetetraacetic acid solution, HeLa cells were counted and digested in 60%

HNO₃ at room temperature overnight. Each sample was diluted with Milli-Q H₂O to obtain 2% HNO₃ solutions. The standards for calibration were freshly prepared by diluting a RuCl₃ stock solution with 2% HNO₃ in Milli-Q H₂O. The ruthenium concentration in each part was determined by inductively coupled plasma-mass spectrometry (ICP-MS).

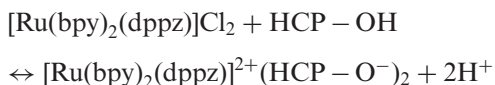
Measurement of the binding affinity of Ru-dppz complex with ctDNA and chlorinated phenols

At least three competing chemical equilibria should be considered, each has its respective binding constant:

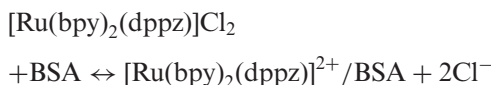
(i) The binding of [Ru(bpy)₂(dppz)]Cl₂ to DNA:



(ii) The anion exchange between [Ru(bpy)₂(dppz)]Cl₂ and chlorophenolate and formation of the ion-pairing complex:



(iii) The binding of [Ru(bpy)₂(dppz)]Cl₂ to bovine serum albumin (BSA)



The absorption titrations of [Ru(bpy)₂(dppz)]Cl₂ in buffer were performed using a fixed concentration (5 μM) for Ru complex to which increments of the DNA stock solution were added. The intrinsic binding constant $K_{b(\text{Ru-DNA})}$, based on the absorption titration, was measured by monitoring the changes in absorption at the MLCT (metal to ligand charge transfer) band with increasing concentration of DNA using the following equation (37):

$$[\text{DNA}]/(\varepsilon_a - \varepsilon_f) = [\text{DNA}]/(\varepsilon_b - \varepsilon_f) + 1/K_{b(\text{Ru-DNA})}(\varepsilon_b - \varepsilon_f) \quad (1)$$

Where [DNA] is the concentration of added DNA in base pairs, ε_a is the apparent absorption coefficient, which was obtained by calculating $A_{\text{abs}}/[\text{Ru}]$, and ε_f and ε_b are the extinction coefficients for the free Ru(II) complex and the Ru(II) complex in the fully bound form, respectively. In a plot of $[\text{DNA}]/(\varepsilon_a - \varepsilon_f)$ versus [DNA], $K_{b(\text{Ru-DNA})}$ is given by the ratio of the slope to the y intercept. Binding constant obtained for [Ru(bpy)₂(dppz)]Cl₂ is $1.5 \times 10^6 \text{ M}^{-1}$ (Supplementary Figure S5), which is consistent with literature report (9,38).

Second, the binding affinity of [Ru(bpy)₂(dppz)]Cl₂ with chlorinated phenols ($K_{b(\text{Ru-HCPs})}$) was measured by fluorescence displacement method using ctDNA. As we know, in aqueous solution, Ru-dppz complexes luminesce brightly only when bound to DNA. So Ru-dppz complex can be used as fluorescent probe here due to the light-switching effect upon interaction with DNA. When chemicals compete to bind Ru-dppz complex from DNA, the luminescence of

Ru-dppz-DNA will decrease. In the binding solution (10 mM Tris-HCl, pH 7.4), ctDNA and Ru-dppz complex were kept at 100 and 50 μM, respectively. Each chemical was added into the pre-incubated ctDNA/Ru-dppz complex solution with varying concentrations. The fluorescence signal was measured after incubation at RT for 10 min. The 50% inhibitory concentration of each chlorinated phenol (IC₅₀) could be obtained from the established competitive titration curve. The dissociation constants and binding constants between each chlorinated phenol and Ru-dppz complex were calculated by the following equation (39):

$$K_d = [IC_{50}]/(1 + [\text{probe}]/K_{\text{probe}(\text{DNA})}) \quad (2)$$

$$K_{b(\text{Ru-HCPs})} = 1/K_d \quad (3)$$

Where [probe] is the concentration of ctDNA (100 μM), the intrinsic ctDNA binding constant $K_{b(\text{Ru-DNA})}$ of [Ru(bpy)₂(dppz)]Cl₂ is $1.5 \times 10^6 \text{ M}^{-1}$. $K_{\text{probe}(\text{DNA})}$ is the dissociation constant for the intercalation of Ru with ctDNA, thus $K_{\text{probe}(\text{DNA})} = 1/1.5 \times 10^6 \text{ M}^{-1}$.

Binding affinity of BSA/Ru-dppz

BSA/Ru-dppz binding analysis ($K_{b(\text{Ru-BSA})}$) was conducted by addition of [Ru(bpy)₂(dppz)]Cl₂ to BSA (5 μM)/warfarin (10 μM) ($K_{b(\text{warfarin-BSA})} = 4.5 \times 10^4 \text{ M}^{-1}$) solution (34,40), resulting in a decrease in warfarin fluorescence, the half inhibitory concentration of Ru-dppz (IC₅₀) could be obtained from the established competitive titration curve. The dissociation constants and binding constants between BSA and Ru-dppz complex were calculated by the following equations (4) and (5):

$$K_d = [IC_{50}]/(1 + [\text{probe}]/K_{\text{probe}(\text{warfarin})}) \quad (4)$$

$$K_{b(\text{Ru-BSA})} = 1/K_d \quad (5)$$

Where [probe] is the concentration of warfarin, the intrinsic warfarin binding constant $K_{b(\text{warfarin-BSA})}$ of BSA is $4.5 \times 10^4 \text{ M}^{-1}$. $K_{\text{probe}(\text{warfarin})}$ is the dissociation constant for the intercalation of warfarin in BSA, here $K_{\text{probe}(\text{warfarin})} = 1/4.5 \times 10^4 \text{ M}^{-1}$.

RESULTS AND DISCUSSION

The most effective nuclear uptake of [Ru(bpy)₂(dppz)]²⁺ is facilitated, unexpectedly, by 2,3,4,5-tetrachlorophenol (2,3,4,5-TeCP), rather than the most-highly chlorinated PCP

As we reported in our recent work, PCP was found to remarkably enhance the cellular and nuclear uptake of cell-impermeable Ru(II)-polypyridyl complexes such as [Ru(bpy)₂(dppz)]Cl₂ via forming lipophilic and relatively stable ion-pair complexes (33). However, it remains unclear whether the enhanced cellular and nuclear uptake of [Ru(bpy)₂(dppz)]²⁺ is only limited to PCP, or it is a general phenomenon for other HCPs. So in this study, cellular and nuclear uptake of the model Ru(II)-dppz complex [Ru(bpy)₂(dppz)]Cl₂ was studied in HeLa cell with three groups of HCPs (six TCPs, three TeCPs and PCP) (Scheme 1).

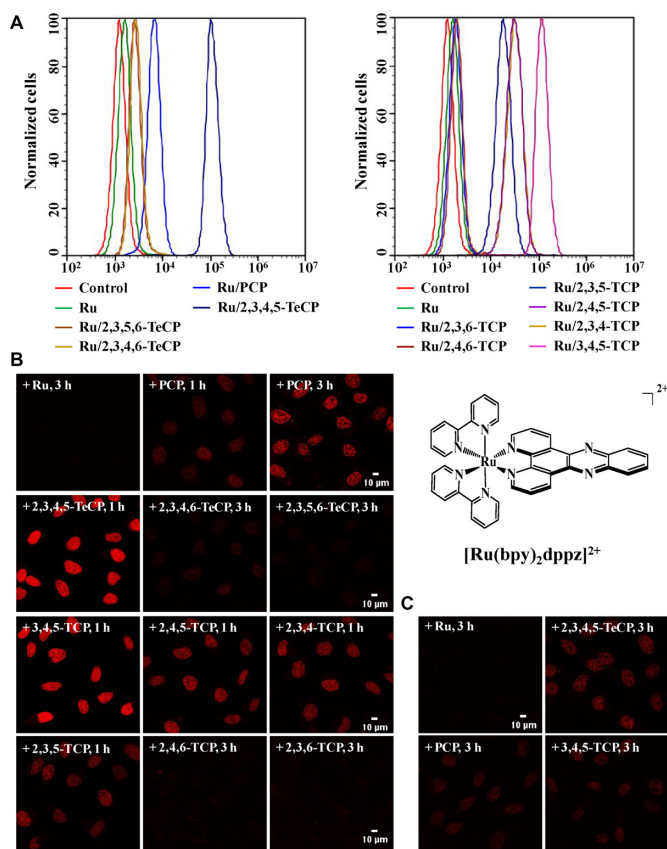


Figure 1. Cellular uptake of $[\text{Ru}(\text{bpy})_2(\text{dppz})]^{2+}$ is markedly enhanced in the presence of HCPs. (A), Flow cytometry analysis of HeLa cells incubated with Ru (100 μM) in the absence or presence of HCPs (300 μM) for 1 h in serum-free medium. Dead cell stain To-Pro-3 (1 μM) was used to exclude or detect dead cells. (B) and (C), Confocal imaging of HeLa cells incubated with Ru (100 μM) in the absence or presence of HCPs (300 μM) in serum-free medium (B) and in full medium (C).

We found that cellular and nuclear uptake of $[\text{Ru}(\text{bpy})_2(\text{dppz})]^{2+}$ can be facilitated by all three groups of HCPs in serum-free medium (only cytoplasmic uptake was observed for 2,4,6- and 2,3,6-TCP) as shown by both flow-cytometry and CLSM (Figure 1A and B). Interestingly and unexpectedly, among all these HCPs tested, 2,3,4,5-TeCP was found to be the most effective one in facilitating nuclear uptake of $[\text{Ru}(\text{bpy})_2(\text{dppz})]^{2+}$, which is even better than the most-highly chlorinated PCP, and much better than its two other TeCP isomers (2,3,4,6- and 2,3,5,6-TeCP) (Figure 1A and B). Cellular or nuclear uptake efficiency was found to follow the general order by luminescence intensity: 2,3,4,5-TeCP > 3,4,5-TCP > 2,3,4-TCP \approx 2,4,5-TCP \approx 2,3,5-TCP > PCP > 2,3,4,6-TeCP \approx 2,3,5,6-TeCP > 2,4,6-TCP \approx 2,3,6-TCP (Supplementary Figure S1). To further determine the cellular and nuclear uptake of Ru by HCPs more accurately, ICP-MS was used to quantify the exact uptake dosage of Ru and similar results were observed as shown in Figure 2. More importantly, nuclear uptake of $[\text{Ru}(\text{bpy})_2(\text{dppz})]^{2+}$ could also be facilitated by 2,3,4,5-TeCP, 3,4,5-TCP and PCP in full medium containing serum (Figure 1C and Supplementary Figure S2).

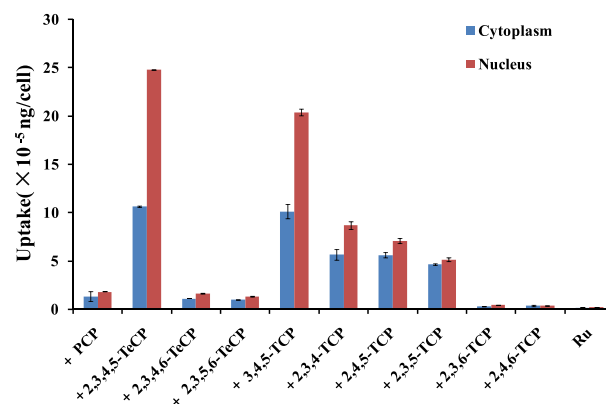


Figure 2. Cellular uptake of $[\text{Ru}(\text{bpy})_2(\text{dppz})]^{2+}$ in the presence of HCPs was determined by ICP-MS. ICP-MS assay for Ru distribution in the cell nucleus and cytoplasm. Cells were treated with Ru (100 μM) in the presence or absence of HCPs (300 μM) for 1 h in serum-free medium. Data represent mean \pm S.D. of three independent experiments.

Then the question is: what are the major physico-chemical factors in determining the nuclear uptake of $[\text{Ru}(\text{bpy})_2(\text{dppz})]^{2+}$ in the presence of HCPs?

The lipophilicity of HCPs is not correlated with the nuclear uptake of $[\text{Ru}(\text{bpy})_2(\text{dppz})]^{2+}$

It has been shown that the uptake efficiency of Ru-dppz was dependent on the nature of the ancillary ligands, where more hydrophobic ancillary ligands such as DIP promote an increased rate of cellular uptake of Ru (16,17). According to our recent report, a neutral, lipophilic and relatively stable ion-pairing complex $[\text{Ru}(\text{bpy})_2(\text{dppz})]^{2+}[\text{PCP}^-]_2$ was formed between PCP and $[\text{Ru}(\text{bpy})_2(\text{dppz})]\text{Cl}_2$ (33), where PCP^- (pentachlorophenolate anion) acts as a counter-anion that modulates nuclear uptake of $[\text{Ru}(\text{bpy})_2(\text{dppz})]^{2+}$ without changing its photophysical property. Therefore, we expected that the uptake efficiency of $[\text{Ru}(\text{bpy})_2(\text{dppz})]^{2+}$ might be dependent on the lipophilicity of HCPs ($\log K_{ow}$ value). But to our surprise, as shown in Table 1 and Supplementary Figure S3, no obvious correlation was observed between the cellular uptake of $[\text{Ru}(\text{bpy})_2(\text{dppz})]^{2+}$ and the lipophilicity of HCPs. This suggests that the lipophilicity of HCPs is probably not a major determining factor for Ru uptake, thus we have to look for other major determining factors.

An inverse correlation is observed between nuclear uptake and the lipophilicity of $[\text{Ru}(\text{bpy})_2(\text{dppz})]^{2+}[\text{HCPs}^-]_2$ ion-pairing complexes

Since lipophilicity of the Ru(II) polypyridyl complexes has been suggested to be a crucial factor in determining Ru cellular uptake (16–18), we expected that the lipophilicity of the ion-pairing complexes $[\text{Ru}(\text{bpy})_2(\text{dppz})]^{2+}[\text{HCPs}^-]_2$ formed between $[\text{Ru}(\text{bpy})_2(\text{dppz})]\text{Cl}_2$ and HCPs might have a good correlation with Ru uptake. Interestingly and surprisingly, an opposite correlation was observed in partitioning studies of the ion-pairing complexes. As we can see from Figures 3 and 4, the lipophilic ion-pairing com-

Table 1. Physicochemical properties of HCPs, cellular uptake of $[\text{Ru}(\text{bpy})_2\text{dppz}]^{2+}$ and the binding constant between $[\text{Ru}(\text{bpy})_2\text{dppz}]\text{Cl}_2$ and HCPs

HCPs	$\text{p}K_{\text{a}}$ (53,54)	$\log K_{\text{ow}}$ (52)	$K_{\text{b}(\text{Ru-HCPs})}/\text{M}^{-1}$	Ru uptake $\times 10^{-5}$ (ng/cell)
PCP	4.74	5.01	$1.49 \pm 0.23 \times 10^5$	3.71 ± 0.48
2,3,5,6-TeCP	5.3	4.90	$2.18 \pm 0.26 \times 10^4$	2.12 ± 0.08
2,3,4,6-TeCP	5.22	4.24	$5.55 \pm 0.30 \times 10^4$	2.30 ± 0.09
2,3,4,5-TeCP	5.64	4.95	$2.94 \pm 0.14 \times 10^5$	34.2 ± 0.09
2,4,6-TCP	5.99	3.69	$1.14 \pm 0.15 \times 10^4$	1.21 ± 0.06
2,3,6-TCP	5.90	3.88	$1.34 \pm 0.17 \times 10^4$	0.82 ± 0.03
2,3,5-TCP	6.43	4.21	$1.35 \pm 0.02 \times 10^4$	11.6 ± 0.05
3,4,5-TCP	7.83	4.39	$>1.38 \pm 0.16 \times 10^5$	29.6 ± 0.75
2,4,5-TCP	7.00	3.72	$1.00 \pm 0.18 \times 10^5$	12.2 ± 0.27
2,3,4-TCP	6.50	4.07	$1.38 \pm 0.28 \times 10^5$	13.0 ± 0.53

Data of $K_{\text{b}(\text{Ru-HCPs})}$ and Ru uptake represent mean \pm S.D. of three independent experiments. $\text{p}K_{\text{a}}$ and $\log K_{\text{ow}}$ values for chlorophenols are from 52–54.

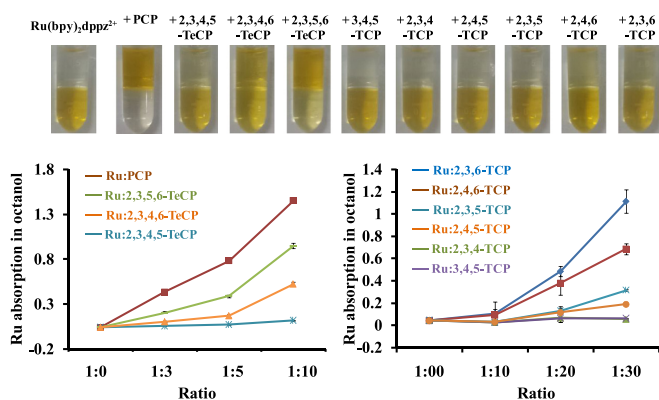


Figure 3. Partitioning studies of $[\text{Ru}(\text{bpy})_2\text{dppz}]\text{Cl}_2$ in the presence of HCPs. Partitioning studies of Ru (100 μM) between n-octanol and aqueous phases (Tris-HCl buffer, 10 mM, pH 7.4) in the presence of HCPs with different ratios were measured. Data represent mean \pm S.D. of three independent experiments.

plexes formed between $[\text{Ru}(\text{bpy})_2(\text{dppz})]\text{Cl}_2$ and 2,3,4,5-TeCP, or with 3,4,5-TCP are the least hydrophobic ion-pairing complexes among the three TeCP isomers and the six TCP isomers, respectively; but the nuclear uptake of $[\text{Ru}(\text{bpy})_2(\text{dppz})]^{2+}$ with 2,3,4,5-TeCP or 3,4,5-TCP are clearly the most effective ones. In clear contrast, although $[\text{Ru}(\text{bpy})_2(\text{dppz})]\text{Cl}_2$ with 2,3,5,6-TeCP and 2,3,4,6-TeCP, or with 2,3,6-TCP and 2,4,6-TCP, are partitioned into the organic phase more effectively, they show much less effective cellular uptake. These results suggest that the least hydrophobic ion-pairing complexes formed between $[\text{Ru}(\text{bpy})_2(\text{dppz})]\text{Cl}_2$ and HCPs will enter the nucleus more effectively than the more hydrophobic ones. In other words, contrary to our expectations, there is an inverse correlation between nuclear uptake and lipophilicity of the ion-pairing complexes $[\text{Ru}(\text{bpy})_2(\text{dppz})]^{2+}[\text{HCPs}^-]_2$ in general (Figure 4).

Our above findings in live-cells are consistent with what Lincoln's group reported previously in fixed cells (22,41). They found that the Ru(II) complexes by substituting with alkyl ether chains of increasing length exhibited distinctly different cellular localization in fixed cells (It should be noted, however, that no nuclear uptake was observed with these ruthenium complexes in live cells) due to their differ-

ent lipophilicity: The least lipophilic complex enters inside the nucleus to stain DNA, while the most lipophilic complex preferentially stains membrane-rich parts of the cell. Therefore, for metal complexes to enter the cell nucleus, the lipophilicity of the complex has to fall within an optimal window, otherwise the complex either becomes too insoluble in aqueous media and can't get through the cell membrane for low lipophilicity, or is trapped within the membrane or in organelles in the cytoplasm if it is highly lipophilic. Based on the above considerations, we speculate that nuclear uptake of cationic metal complexes may favor toward those with lower lipophilicity, provided they can first penetrate through the cytoplasmic membrane. Therefore, there should be other crucial physicochemical parameters in determining nuclear uptake of the cationic metal complexes via ion-pairing with the counter-anions.

The enhanced nuclear uptake of $[\text{Ru}(\text{bpy})_2(\text{dppz})]^{2+}$ by HCPs is positively correlated with the binding stability of the ion-pairing complexes formed between $[\text{Ru}(\text{bpy})_2(\text{dppz})]\text{Cl}_2$ and HCPs

After considering the lipophilicity for both HCPs and the formed ion-pairing complexes, we then investigated another potential important factor crucial for the nuclear uptake, the binding stability ($K_{\text{b}(\text{Ru-HCPs})}$) between $[\text{Ru}(\text{bpy})_2(\text{dppz})]\text{Cl}_2$ and HCPs.

As we reported recently, ion pairs were found to be formed between PCP and Ru(II) complexes, which were held together mainly by Coulombic forces (33). For Ru(II) complex, to escape being trapped by protein and membrane structures in the cytoplasm to get into the nucleus, ion pair formed with HCPs should be neutral and stable enough. In other word, the binding affinity between HCPs and Ru(II) complex should be strong enough to keep the ion-pairing complex as a whole before reaching nucleus. Therefore, we speculate that the binding affinity between HCPs and Ru(II) complex should be another critical physicochemical factor in determining cellular uptake and distribution of Ru(II) complex. To test the above hypothesis, the binding constants ($K_{\text{b}(\text{Ru-HCPs})}$) between $[\text{Ru}(\text{bpy})_2(\text{dppz})]\text{Cl}_2$ and HCPs were measured by fluorescence displacement method (Supplementary Figure S4, for details, see 'Materials and Methods' section).

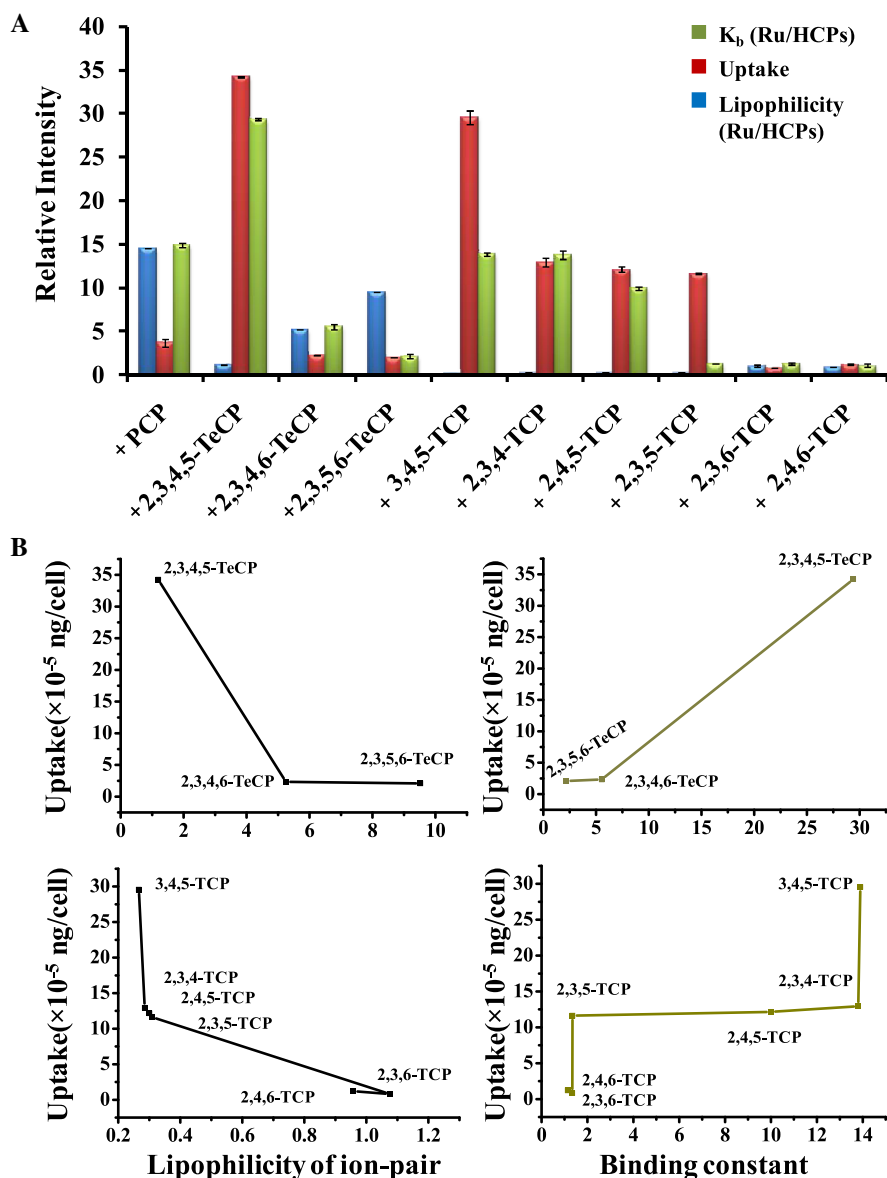


Figure 4. Correlations of nuclear uptake of $[\text{Ru}(\text{bpy})_2(\text{dppz})]^{2+}$ in the presence of HCPs with binding stability and hydrophobicity of the formed ion-pairing complexes $[\text{Ru}(\text{bpy})_2(\text{dppz})]^{2+}[\text{HCPs}^-]_2$. (A), (red bar) nuclear uptake of Ru ($\times 10^{-5}$ ng/cell) was determined by ICP-MS; (green bar) binding ability ($\times 10^4 \text{ M}^{-1}$) was measured by fluorescence displacement method; (blue bar) The lipophilicity of the formed ion-pairing complexes were determined by partitioning studies (data obtained by absorption intensity (Ru/HCPs = 1:10) in n-octanol phase $\times 10$). (B), correlation between nuclear uptake and binding constant (positive correlation)/lipophilicity (inverse correlation) of the formed ion-pairing complexes. Data represent mean \pm S.D. of three independent experiments.

As expected, the nuclear uptake of $[\text{Ru}(\text{bpy})_2(\text{dppz})]^{2+}$ by HCPs was found to be positively correlated with the binding ability between $[\text{Ru}(\text{bpy})_2(\text{dppz})]\text{Cl}_2$ and HCPs (Figure 4 and Table 1). Interestingly, in the competition experiment, we found that the four HCPs (including 2,3,4,5-TeCP, 3,4,5-, 2,3,4- and 2,4,5-TCP) showing the high efficiency in facilitating nuclear uptake could also cause blue shift of Ru emission spectrum in the DNA system when the concentrations of the four HCPs are relatively high (Supplementary Figure S4), which indicate that new ternary complexes are probably formed among $[\text{Ru}(\text{bpy})_2(\text{dppz})]\text{Cl}_2$, DNA and the four HCPs.

Then the question is what is the possible underlying molecular basis for the different Ru(II)-binding affinity for these chlorophenol isomers (TeCPs; TCPs)?

As we recently reported, a neutral, lipophilic and relatively stable ion-pairing complex was formed between Ru(II) complex and PCP with a 1:2 stoichiometry as demonstrated by single-crystal X-ray diffraction (33). The ion-pairing complex has been suggested to belong to the outer sphere contact ion-pair (42), in which the coordinatively saturated first coordination sphere of the cation (Ru(II) complex) is no longer accessible to the anion (pentachlorophenolate), and consequently, the anion is relegated

to the second coordination sphere, interacting with the cation through electrostatic and other weak forces such as aromatic pi stacking, H-bonding, δ - δ , CH- δ , etc (42–46). According to the crystal structure, solvent water molecules were also found to interact with the phenolic hydroxyl group by forming hydrogen bond, which appears to be one of the major forces in holding the ion-pairing complex together (33).

Hence, based on the chemical structures of chlorophenol isomers, the strength of the binding affinity ($K_{b(\text{Ru-HCPs})}$) between Ru(II) complex and HCPs might be determined by the basic physicochemical properties of chlorophenols (47–50), which include the electron-withdrawing properties of Cl atoms and the steric hindrance effects as listed below: (i) electron-withdrawing Cl-substituents at both ortho-positions (2- and 6-positions) reduce the π -electron density in aromatic ring, and as a result, leading to weak electrostatic forces; (ii) Cl-substituents at both ortho-positions (2- and 6-positions) enhance steric hindrance effects, and reduce chances for solvent water molecules interacting with the phenolic hydroxyl group. For the three TeCP isomers, their Ru(II)-binding affinity strength follows the order: 2,3,4,5-TeCP \gg 2,3,4,6-TeCP $>$ 2,3,5,6-TeCP. Comparing with 2,3,4,5-TeCP with only one Cl atom at 2-position, both Cl-substituents at two ortho-positions (2- and 6-positions) for 2,3,4,6-TeCP and 2,3,5,6-TeCP will enhance the steric hindrance effects; on the other hand, the electron withdrawing Cl-substitution groups at two ortho-positions also reduce the π -electron density in the aromatic ring, which, consequently, weakens the electrostatic forces formed between solvent H₂O molecules and the phenolic hydroxyl group of HCP; While only one Cl-substituent in 2-position for 2,3,4,5-TeCP makes a higher π -electron density in the aromatic ring, thus leading to a relatively stronger electrostatic force. Similar explanations may also be applied to the six TCP isomers: 2,3,6-TCP, 2,4,6-TCP with Cl-substituents at two ortho-positions (2- and 6-positions) have both stronger steric hindrance effects and lower π -electron density, which contribute to their lower Ru(II)-binding constant K values for the two TCPs than that for the other four TCPs (Table 1).

The binding affinity ($K_{b(\text{Ru-BSA})}$) between $[\text{Ru}(\text{bpy})_2(\text{dppz})]\text{Cl}_2$ and BSA is determined by fluorescence displacement method

Since Ru luminescence was also observed in the cytoplasm, which is probably caused by interaction with cytoplasmic proteins (40,51), we further studied the binding affinity between $[\text{Ru}(\text{bpy})_2(\text{dppz})]\text{Cl}_2$ and BSA, a structural homologue of human serum albumin (HSA), by fluorescence displacement method, where warfarin was used as the fluorescent probe (for details, see 'Materials and Methods' section). As shown in Supplementary Figure S5, interactions between $[\text{Ru}(\text{bpy})_2(\text{dppz})]\text{Cl}_2$ and BSA indeed exist, and the binding constant ($K_{b(\text{Ru-BSA})}$) between $[\text{Ru}(\text{bpy})_2(\text{dppz})]\text{Cl}_2$ and BSA was determined to be $9.78 \times 10^4 \text{ M}^{-1}$, which is much higher than the binding constants ($K_{b(\text{Ru-HCPs})}$) of the ion-pairing complexes formed between $[\text{Ru}(\text{bpy})_2(\text{dppz})]\text{Cl}_2$ and 2,4,6-TCP or 2,3,6-TCP ($1.14 \times 10^4 \text{ M}^{-1}$, $1.34 \times 10^4 \text{ M}^{-1}$, respectively). The relatively weak Ru(II)-binding affinity for 2,4,6-TCP, 2,3,6-TCP and 2,3,5-

TeCP makes the ion-pairs formed not strong enough to compete with protein or even membrane components in the cytoplasm (or in full medium containing serum), thus leading to poor nuclear uptake of $[\text{Ru}(\text{bpy})_2(\text{dppz})]^{2+}$. Analogous effects were observed for 2,3,4,6-TeCP or 2,3,5,6-TeCP. In clear contrast, the relatively strong Ru(II)-binding affinity for 2,3,4,5-TeCP ($2.94 \times 10^5 \text{ M}^{-1}$) and 3,4,5-TCP ($>1.38 \times 10^5 \text{ M}^{-1}$) makes the ion-pairing complexes formed strong enough to compete with cytoplasmic components, resulting in efficient nuclear uptake of $[\text{Ru}(\text{bpy})_2(\text{dppz})]^{2+}$ even in full medium. Therefore, strong binding affinity ($K_{b(\text{Ru-HCPs})}$) between $[\text{Ru}(\text{bpy})_2(\text{dppz})]\text{Cl}_2$ and HCPs is assumed to be one of the most important factors in determining whether $[\text{Ru}(\text{bpy})_2(\text{dppz})]\text{Cl}_2/\text{HCPs}$ could make its way through to the nucleus. These results further confirm that the ion-pairing complex formed should be neutral and stable enough to escape being trapped by protein and membrane structures in the cytoplasm or in full medium to enter the nucleus.

The enhanced nuclear uptake efficiency of $[\text{Ru}(\text{bpy})_2(\text{dppz})]^{2+}$ by HCPs is determined by a combination of both of the binding affinity and the lipophilicity of the formed ion-pairing complex

After considering all the potential factors, the uptake efficiency of $[\text{Ru}(\text{bpy})_2(\text{dppz})]^{2+}$ by all three groups of HCPs (TCPs, TeCPs and PCP) can be well explained by the combination effects of both the binding affinity and the lipophilicity of the formed ion-pairing complexes. In general, (i) the cellular uptake efficiency follows the following order: 2,3,4,5-TeCP, 3,4,5-TCP $>$ 2,3,4-TCP, 2,4,5-TCP, 2,3,5-TCP $>$ PCP $>$ 2,3,4,6-TeCP, 2,3,5,6-TeCP $>$ 2,4,6-TCP, 2,3,6-TCP; (ii) the binding affinity of the ion-pairing complexes follows the similar order: 2,3,4,5-TeCP, PCP, 3,4,5-TCP $>$ 2,3,4-TCP $>$ 2,4,5-TCP $>$ 2,3,4,6-TeCP $>$ 2,3,5,6-TeCP $>$ 2,3,5-TCP $>$ 2,3,6-TCP $>$ 2,4,6-TCP; while in contrast, (iii) the lipophilicity of the ion-pairing complexes follows an opposite order: 2,3,4,5-TeCP $<$ 2,3,4,6-TeCP $<$ 2,3,5,6-TeCP, PCP; 3,4,5-TCP $<$ 2,3,4-TCP $<$ 2,4,5-TCP $<$ 2,3,5-TCP $<$ 2,4,6-TCP $<$ 2,3,6-TCP (Table 1 and Figure 4). These results clearly demonstrate that the nuclear uptake of $[\text{Ru}(\text{bpy})_2(\text{dppz})]^{2+}[\text{HCPs}^-]_2$ is positively correlated with their binding ability, however, inversely correlated with their lipophilicity. So the enhanced nuclear uptake efficiency of $[\text{Ru}(\text{bpy})_2(\text{dppz})]^{2+}$ by HCPs is, to a large extent, determined by a combination effect of their binding affinity and the lipophilicity of the ion-pairing complexes $[\text{Ru}(\text{bpy})_2(\text{dppz})]^{2+}[\text{HCPs}^-]_2$.

For 2,3,4,5-TeCP, the highest Ru(II)-binding constant value ($2.94 \times 10^5 \text{ M}^{-1}$), along with the low lipophilicity of the formed ion-pairing complex $[\text{Ru}(\text{bpy})_2(\text{dppz})]^{2+}[2,3,4,5\text{-TeCP}^-]_2$ together contributes to its most effective nuclear uptake of $[\text{Ru}(\text{bpy})_2(\text{dppz})]^{2+}$. In contrast, for 2,4,6-TCP and 2,3,6-TCP, their high lipophilicity of formed ion-pairs would make them easily be trapped in the lipid membrane structures or proteins in cytoplasm, and their lowest Ru(II)-binding constant K values ($1.14 \times 10^4 \text{ M}^{-1}$ and $1.34 \times 10^4 \text{ M}^{-1}$, respectively) among all HCPs tested would let them be readily dissociated in the environment full of competing bio-molecules. As for PCP, although its Ru(II)-binding

affinity ($1.49 \times 10^5 \text{ M}^{-1}$) is relatively high, the ion-pairing complex $[\text{Ru}(\text{bpy})_2(\text{dppz})]^{2+}[\text{PCP}^-]_2$ formed is the most lipophilic one among all HCPs tested as we can see in the partitioning study (Figure 3). The property with the highest hydrophobicity, on one hand, makes it too insoluble in aqueous media: much more precipitation was observed when $[\text{Ru}(\text{bpy})_2(\text{dppz})]\text{Cl}_2$ was mixed together with PCP than that with other HCPs (Supplementary Figure S6); on the other hand, it might also be much easily trapped within the lipid bi-layer membrane or organelle membrane structures in the cytoplasm. So all the above results could explain the phenomenon that Ru uptake efficiency for PCP is much poorer than for 2,3,4,5-TeCP and even poorer than that for the four TCPs (3,4,5-TCP, 2,3,5-TCP, 2,3,4-TCP, 2,4,5-TCP). The relatively poor Ru uptake efficiency for 2,3,4,6-TeCP and 2,3,5,6-TeCP can also attribute to their relatively high hydrophobicity and relatively low binding affinity after forming ion-pairs with $[\text{Ru}(\text{bpy})_2(\text{dppz})]\text{Cl}_2$.

Above all, the binding affinity and the lipophilicity of the formed ion-pairing complexes are two major physico-chemical factors in determining nuclear uptake efficiency of Ru: the higher Ru-binding affinity, the better Ru uptake efficiency; while in contrast, the higher lipophilicity of the formed ion-pairing complexes leads to the poorer Ru uptake efficiency.

CONCLUSIONS

In conclusion, we have shown that the Ru(II)-dppz polypyridyl ‘light switch’ complex $[\text{Ru}(\text{bpy})_2(\text{dppz})]\text{Cl}_2$ was readily taken up by cells and preferentially localized in the nucleus in the presence of three groups of HCPs (TCPs, TeCPs and PCP), via forming neutral, lipophilic and relatively stable ion-pair complexes. HCPs here act as counter-anions modulating cellular and nuclear uptake of Ru(II)-dppz complexes yet without changing the DNA ‘light switch’ nature of Ru(II) complexes. The detailed studies demonstrate that both the binding affinity and lipophilicity of the formed ion-pairing complexes are critical physicochemical factors in determining Ru nuclear uptake efficiency by HCPs. The Ru uptake is positively correlated with their binding ability, but inversely correlated with the lipophilicity of the ion-pairing complexes formed. These findings should provide important new perspectives for future investigations on delivering other bioactive metal complexes into their intended cellular targets via ion-pairing method, which is a conceptual breakthrough from the traditional delivering methods.

SUPPLEMENTARY DATA

Supplementary Data are available at NAR Online.

FUNDING

Strategic Priority Research Program of CAS [XDB01020300]; “From 0 to 1” Original Innovation Project, the Basic Frontier Scientific Research Program, CAS [ZDBS-LY-SLH027]; NSF China Grants [21836005, 21577149, 21477139, 21621064, 21407163, 21777180]; NIH Grants [ES11497, RR01008, ES00210]; Fundamental

Research Funds for the Central Universities [18zxxxt38, 2018A030310242]. Funding for open access charge: NSFC Grants

Conflict of interest statement. None declared.

REFERENCES

1. Wang, D. and Lippard, S.J. (2005) Cellular processing of platinum anticancer drugs. *Nat. Rev.*, **4**, 302–320.
2. Spreckelmeyer, S., Orvig, C. and Casini, A. (2014) Cellular transport mechanisms of cytotoxic metalodrugs: an overview beyond cisplatin. *Molecules*, **19**, 15584–15610.
3. Zeng, L.L., Gupta, P., Chen, Y.L., Wang, E.J., Ji, L.N., Chao, H. and Chen, Z.S. (2017) The development of anticancer ruthenium(II) complexes: from single molecule compounds to nanomaterials. *Chem. Soc. Rev.*, **46**, 5771–5804.
4. Zhao, Q., Huang, C.H. and Li, F.Y. (2011) Phosphorescent heavy-metal complexes for bioimaging. *Chem. Soc. Rev.*, **40**, 2508–2524.
5. Viogradova, E.V., Zhang, C., Spokoyny, A.M., Pentelute, B.L. and Buchwald, S.L. (2015) Organometallic palladium reagents for cysteine bioconjugation. *Nature*, **526**, 687–691.
6. Saha, M.L., Yan, X. and Stang, P.J. (2016) Photophysical properties of organoplatinum(II) compounds and derived self-assembled metallacycles and metallacages: fluorescence and its applications. *Acc. Chem. Res.*, **49**, 2527–2539.
7. Liu, L.J., Wang, W.H., Huang, S.Y., Hong, Y.J., Li, G.D., Lin, S., Tian, J.L., Cai, Z.W., Wang, H.M. David, Ma, D.L. *et al.* (2017) Inhibition of the Ras/Raf interaction and repression of renal cancer xenografts in vivo by an enantiomeric iridium(III) metal-based compound. *Chem. Sci.*, **8**, 4756–4763.
8. Vellaisamy, K., Li, G.D., Ko, C.N., Zhong, H.J., Fatima, S., Kwan, H.Y., Wong, C.Y., Kwong, W.J., Tan, W.H., Leung, C.H. *et al.* (2018) Cell imaging of dopamine receptor using agonist labeling iridium(III) complex. *Chem. Sci.*, **9**, 1119–1125.
9. Friedman, A.E., Chambron, J.C., Sauvage, J.P., Turro, N.J. and Barton, J.K. (1990) Molecular light switch for DNA - $[\text{Ru}(\text{bpy})_2(\text{dppz})]^{2+}$. *J. Am. Chem. Soc.*, **112**, 4960–4962.
10. Neugebauer, U., Pellegrin, Y., Devocelle, M., Forster, R.J., Signac, W., Morand, N. and Keyes, T.E. (2008) Ruthenium polypyridyl peptide conjugates: membrane permeable probes for cellular imaging. *Chem. Commun.*, 5307–5309.
11. Whitemore, T.J., White, T.A. and Turro, C. (2018) New ligand design provides delocalization and promotes strong absorption throughout the visible region in a Ru(II) complex. *J. Am. Chem. Soc.*, **140**, 229–234.
12. Pierroz, V., Joshi, T., Leonidova, A., Mari, C., Schur, J., Ott, I., Spiccia, L., Ferrari, S. and Gasser, G. (2012) Molecular and cellular characterization of the biological effects of ruthenium complexes incorporating 2-pyridyl-2-pyrimidine-4-carboxylic acid. *J. Am. Chem. Soc.*, **134**, 20376–20387.
13. Mari, C., Pierroz, V., Ferrari, S. and Gasser, G. (2015) Combination of ruthenium complexes and light: new frontiers in cancer therapy. *Chem. Sci.*, **6**, 2660–2686.
14. Knoll, J.D. and Turro, C. (2015) Control and utilization of ruthenium and rhodium metal complex excited states for photoactivated cancer therapy. *Coord. Chem. Rev.*, **282–283**, 110–126.
15. Liu, Z. and Sadler, P.J. (2014) Organoiridium complexes: anticancer agents and catalysts. *Acc. Chem. Res.*, **47**, 1174–1185.
16. Puckett, C.A. and Barton, J.K. (2007) Methods to explore cellular uptake of ruthenium complexes. *J. Am. Chem. Soc.*, **129**, 46–47.
17. Puckett, C.A. and Barton, J.K. (2008) Mechanism of cellular uptake of a ruthenium polypyridyl complex. *Biochemistry*, **47**, 11711–11716.
18. Komor, A.C. and Barton, J.K. (2013) The path for metal complexes to a DNA target. *Chem. Commun.*, **49**, 3617–3630.
19. Hartshorn, R.M. and Barton, J.K. (1992) Novel dipyrrophenazine complexes of Ruthenium(II) - exploring luminescent reporters of DNA. *J. Am. Chem. Soc.*, **114**, 5919–5925.
20. Lo, K.K.W., Lee, T.K.M., Lau, J.S.Y., Poon, W.L. and Cheng, S.H. (2008) Luminescent biological probes derived from ruthenium(II) estradiol polypyridine complexes. *Inorg. Chem.*, **47**, 200–208.
21. Puckett, C.A. and Barton, J.K. (2009) Fluorescein redirects a ruthenium-octaarginine conjugate to the nucleus. *J. Am. Chem. Soc.*, **131**, 8738–8739.

22. Svensson, F.R., Matson, M., Li, M. and Lincoln, P. (2010) Lipophilic ruthenium complexes with tuned cell membrane affinity and photoactivated uptake. *Biophys. Chem.*, **149**, 102–106.
23. Svensson, F.R., Abrahamsson, M., Stromberg, N., Ewing, A.G. and Lincoln, P. (2011) Ruthenium(II) complex enantiomers as cellular probes for diastereomeric interactions in confocal and fluorescence lifetime imaging microscopy. *J. Phys. Chem. Lett.*, **2**, 397–401.
24. Zhu, B.Z. and Chevion, M. (2000) Mechanism of the synergistic cytotoxicity between pentachlorophenol and copper-1,10-phenanthroline complex: the formation of a lipophilic ternary complex. *Chem. Biol. Interact.*, **129**, 249–261.
25. Levy, S., Shechtman, S., Zhu, B.Z., Stadtman, E.R., Stadler, R. and Chevion, M. (2007) Synergism between the toxicity of chlorophenols and iron complexes. *Environ. Toxicol. Chem.*, **26**, 218–224.
26. Zhu, B.Z., Kalyanaraman, B. and Jiang, G.B. (2007) Molecular mechanism for metal-independent production of hydroxyl radicals by hydrogen peroxide and halogenated quinones. *Proc. Natl. Acad. Sci. U.S.A.*, **104**, 17575–17578.
27. Zhu, B.Z., Mao, L., Huang, C.H., Qin, H., Fan, R.M., Kalyanaraman, B. and Zhu, J.G. (2012) Unprecedented hydroxyl radical-dependent two-step chemiluminescence production by polyhalogenatedquinoid carcinogens and H₂O₂. *Proc. Natl. Acad. Sci. U.S.A.*, **109**, 16046–16051.
28. Sheng, Z.G., Li, Y., Fan, R.M., Chao, X.J. and Zhu, B.Z. (2013) Lethal synergism between organic and inorganic wood preservatives via formation of an unusual lipophilic ternary complex. *Toxicol. Appl. Pharm.*, **266**, 335–344.
29. Shao, J., Huang, C.H., Kalyanaraman, B. and Zhu, B.Z. (2013) Potent methyl oxidation of 5-methyl-2'-deoxycytidine by halogenated quinoidcarcinogens and hydrogen peroxide via a metal-independent mechanism. *Free Radic. Biol. Med.*, **60**, 177–182.
30. Yin, R., Zhang, D., Song, Y., Zhu, B.Z. and Wang, H. (2013) Potent DNA damage by polyhalogenatedquinoid carcinogens and H₂O₂ via a metal-independent and intercalation-enhanced oxidation mechanism. *Sci. Rep.*, **3**, 1269.
31. Fan, R.M., Zhu, B.Z., Huang, C.P., Sheng, Z.G., Mao, L. and Li, M.X. (2016) Different modes of synergistic toxicities between metam/copper (II) and metam/zinc (II) in HepG2 cells: apoptosis vs. necrosis. *Environ. Toxicol.*, **31**, 1964–1973.
32. Shao, B., Mao, L., Qu, N., Wang, Y.F., Gao, H.Y., Li, F., Qin, L., Shao, J., Huang, C.H., Xu, D. et al. (2017) Mechanism of synergistic DNA damage induced by the hydroquinone metabolite of brominated phenolic environmental pollutants and Cu(II): Formation of DNA-Cu complex and site-specific production of hydroxyl radicals. *Free Radic. Biol. Med.*, **104**, 54–63.
33. Zhu, B.Z., Chao, X.J., Huang, C.H. and Li, Y. (2016) Delivering the cell-impermeable DNA 'light-switching' Ru(II) complexes preferentially into live-cell nucleus via an unprecedented ion-pairing method. *Chem. Sci.*, **7**, 4016–4023.
34. Amouyal, E., Homsy, A., Chambron, J.C. and Sauvage, J.P. (1990) Synthesis and study of a mixed-ligand ruthenium(II) complex in its ground and excited-states - bis(2,2'-bipyridine)(dipyrido[3,2-a,2',3'-C]phenazine-N₄N₅)ruthenium(II). *J. Chem. Soc. Dalton.*, **6**, 1841–1845.
35. Sullivan, B.P., Salmon, D.J. and Meyer, T.J. (1978) Mixed phosphine 2,2'-bipyridine complexes of ruthenium. *Inorg. Chem.*, **17**, 3334–3341.
36. Yamada, M., Tanaka, Y., Yoshimoto, Y., Kuroda, S. and Shimao, I. (1992) Synthesis and properties of diamino-substituted dipyrido[3,2-a,2',3'-C]phenazine. *B. Chem. Soc. Jpn.*, **65**, 1006–1011.
37. Wolfe, A., Shimer, G.H. and Meehan, T. (1987) Polycyclic aromatic hydrocarbons physically intercalate into duplex regions of denatured DNA. *Biochemistry*, **26**, 6392–6396.
38. Gill, M.R. and Thomas, J.A. (2009) Ruthenium polypyridyl complexes and DNA -from structural probes to cellular imaging and therapeutics. *Chem. Soc. Rev.*, **41**, 3179–3192.
39. Cheng, Y. and Prusoff, W.H. (1973) Relationship between inhibition constant (K_i) and concentration of inhibitor which causes 50 per cent inhibition (IC₅₀) of an enzymatic-reaction. *Biochem. Pharmacol.*, **22**, 3099–3108.
40. Mandula, H., Parepally, J.M.R., Feng, R. and Smith, Q.R. (2006) Role of site-specific binding to plasma albumin in drug availability to brain. *J. Pharmacol. Exp. Ther.*, **317**, 667–675.
41. Matson, M., Svensson, F.R., Nordén, B. and Lincoln, P. (2011) Correlation between cellular localization and binding preference to RNA, DNA, and phospholipid membrane for luminescent ruthenium(II) complexes. *J. Phys. Chem. B*, **115**, 1706–1711.
42. Macchioni, A. (2005) Ion pairing in transition-metal organometallic chemistry. *Chem. Rev.*, **105**, 2039–2073.
43. Marcus, Y. and Hefter, G. (2006) Ion pairing. *Chem. Rev.*, **106**, 4585–4621.
44. Brak, K. and Jacobsen, E.N. (2013) Asymmetric ion-pairing catalysis. *Angew. Chem. Int. Ed.*, **52**, 534–561.
45. Neubert, R. (1989) Ion-pair transport across membranes. *Pharm. Res.*, **6**, 743–747.
46. Song, I.S., Choi, M.K., Shim, W.S. and Shim, C.K. (2013) Transport of organic cationic drugs: Effect of ion-pair formation with bile salts on the biliary excretion and pharmacokinetics. *Pharmacol. Ther.*, **138**, 142–154.
47. Gao, H.Y., Mao, L., Li, F., Xie, L.N., Huang, C.H., Shao, J., Shao, B., Kalyanaraman, B. and Zhu, B.Z. (2017) Mechanism of intrinsic chemiluminescence production from the degradation of persistent chlorinated phenols by Fenton system: A structure-activity relationship study and the critical role of quinoid and semiquinone radical intermediates. *Environ. Sci. Technol.*, **51**, 2934–2943.
48. Gao, H.Y., Mao, L., Shao, B., Huang, C.H. and Zhu, B.Z. (2016) Why does 2,3,5,6-tetrachlorophenol generate the strongest intrinsic chemiluminescence among all nineteen chlorophenolic persistent organic pollutants during environmentally-friendly advanced oxidation process? *Sci. Rep.*, **6**, 33159.
49. Zhu, B.Z., Shen, C., Gao, H.Y., Zhu, L.Y., Shao, J. and Mao, L. (2017) Intrinsic chemiluminescence production from the degradation of haloaromatic pollutants during environmentally-friendly advanced oxidation processes: mechanism, structure-activity relationship and potential applications. *J. Environ. Sci.*, **62**, 68–83.
50. Zhu, B.Z., Zhu, J.G., Fan, R.M. and Mao, L. (2011) Metal-independent pathways of chlorinated phenol/quinone toxicity. In: Fishbein, J.C. (ed) *Advances in Molecular Toxicology*. Elsevier Science, pp. 1–43.
51. Wragg, A., Gill, M.R., McKenzie, L., Glover, C., Mowll, R., Weinstein, J.A., Su, X.D., Smythe, C. and Thomas, J.A. (2015) Serum albumin binding inhibits nuclear uptake of luminescent metal-complex-based DNA imaging probes. *Chem. Eur. J.*, **21**, 11865–11871.
52. Hansch, C. and Leo, A. (1979) *Substituent Constants for Correlation Analysis in Chemistry and Biology*. John Wiley & Sons, NY.
53. Valdez, C.A. and Leif, R.N. (2015) Chemical tagging of chlorinated phenols for their facile detection and analysis by NMR spectroscopy. *Anal. Bioanal. Chem.*, **407**, 3539–3543.
54. Argese, E., Bettiol, C., Giurin, G. and Miana, P. (1999) Quantitative structure-activity relationships for the toxicity of chlorophenols to mammalian submitochondrial particles. *Chemosphere*, **38**, 2281–2292.